Rare Metal Materials and Engineering
Volume 55, Issue 5, May 2026
Available online at www.rmme.ac.cn

Science Press

Cite this article as: Zhang Tongdi, Ma Sa, Zhong Jing, et al. Three-Dimensional Phase-Field Simulation of Grain Evolution in Physical Vapor Deposited Pure Ti Thin Film[J]. Rare Metal Materials and Engineering, 2026, 55(05): 1137-1145. DOI: https://doi.org/10.12442/j.issn.1002-185X.20250211.

ARTICLE

Three-Dimensional Phase-Field Simulation of Grain Evolution in Physical Vapor Deposited Pure Ti Thin Film

Zhang Tongdi[1], Ma Sa[1,2], Zhong Jing[1], Yang Shenglan[1,3], Zhang Lijun[1]

[1] State Key Laboratory of Powder Metallurgy, Central South University, Changsha 410083, China; [2] School of Materials Science and Engineering, Zhejiang University, Hangzhou 310027, China; [3] National Engineering Research Center for Magnesium Alloys, Chongqing University, Chongqing 400044, China

Abstract: Combining the phase-field method and the moving boundary method, a three-dimensional phase-field simulation was conducted for the growth and grain evolution of Ti films deposited by physical vapor deposition under different deposition rates and grain orientations. The evolution of grain morphology and grain orientation was also taken into consideration. Simulation results show that at lower deposition rates, the surface of the formed Ti film exhibits a distinct oriented texture structure. The surface roughness of the Ti film is positively correlated with the grain misorientation. Moreover, the surface roughness obtained from the simulation is in good agreement with the experiment results.

Key words: physical vapor deposition; phase-field simulation; grain evolution; polycrystalline; Ti thin film

1 Introduction

Physical vapor deposition (PVD) technique is a vitally important technique in the coating fabrication because of its lower processing temperature and eco-friendly nature[1–5]. It is widely used to deposit thin films on substrates in functional applications, such as tools, decorative pieces, and molds. Ti thin film has attracted much attention over the last decades owing to its high mechanical strength, good adhesion strength, fine corrosion resistance, and intrinsic biocompatibility[6–7]. Moreover, PVD can be used to reproducibly prepare nanometer-scale Ti thin film with adjustable surface roughness and well-defined surface topography while maintaining the surface chemical characteristics[8]. Thus, PVD Ti thin films have enormous potential in many applications, including medical implants, micro-electro mechanical systems, as well as nuclear power systems[9–10]. However, in practical applications, the crystallographic orientation of polycrystalline Ti thin film has a significant influence on material properties. For instance, the polycrystalline Ti thin films have been extensively used as the intermediate layer between various coatings and substrates, and thus, a preferred crystallographic orientation or texture of the deposited Ti thin films can directly affect the characteristics of the formed layers[11–12]. Besides, the crystallographic orientation is also a crucial factor for improving the properties of magnetic metallic films and piezoelectric layers[13–14]. Therefore, a comprehensive study on the crystallographic orientation or grain evolution of PVD Ti thin films should be of great importance for tuning their properties/performance.

For the past few years, the crystals and morphologies of Ti thin films fabricated by different PVD techniques have been experimentally studied with some advanced characterization methods[11–19]. Fazio et al[12] found that the crystal structure of Ti films deposited on single-crystal Si (100) is relevant to the film thickness. The film structure may change from face-centered cubic structure to close-packed hexagonal structure with a grain orientation preference along the [100] direction when the film thickness reaches a critical value. Moreover, Gablech et al[11] optimized the deposition parameters for preparing polycrystalline Ti films with desired preferential orientation and ultralow surface roughness, and the residual

Received date: May 24, 2025
Foundation item: National MCF Energy R&D Program of China (2018YFE0306100); Natural Science Foundation of Hunan Province for Distinguished Young Scholars (2021JJ10062); National Natural Science Foundation of China (52101028); China Postdoctoral Science Foundation (2021M703628)
Corresponding author: Zhang Lijun, Ph. D., Professor, State Key Laboratory of Powder Metallurgy, Central South University, Changsha 410083, P. R. China, E-mail: lijun.zhang@csu.edu.cn

stress could be modulated by controlling the crystallographic orientation[19]. However, the microstructure is directly decided by the complex deposited conditions, i.e., substrate material, temperature, angle of incidence, deposition rate, vacuum, and working gas purity. Thus, it is still impossible to rely solely on experiments to explore such a sophisticated relation between PVD conditions and the crystallographic orientation. Moreover, intuitive descriptions of the grain growth and the evolution of grain boundaries are also rarely considered.

Nowadays, the phase-field method is an efficient tool to numerically describe the microstructure evolution of thin films[20–34]. Several studies have focused on the effects of model parameters on the porosity and the evolution of grain orientation for single-phase polycrystalline thin films employing the phase-field method[20–22]. As mentioned above, most thin films consist of multiple small domains varying from nanometers to microns in size, and the tiny domains differ in grain orientation and/or crystal structure. It is essential to describe the evolution of grains and grain boundaries during PVD, which is typically neglected in most research. Fortunately, Stewart et al[35–36] proposed a phase-field model that can simultaneously simulate the surface grain evolution and film growth process of polycrystalline thin films for isotropic single-phase materials prepared by PVD. However, Stewart et al[35–36] used the dimensionless parameters to simplify the numerical process. Therefore, a quantitative description of microstructure evolution is rarely presented. Recently, based on more than 200 sets of microstructure evolution results obtained by phase-field simulations, Yang et al[2] quantitatively established the relationship among the process parameters (deposition rate) and the phase-field model parameters, and the effects of the deposition rate on the microstructure evolution and surface roughness of PVD Mo and Ti films were further evaluated. After that, Dai et al[4] focused on the process parameters for extensively used PVD TiN thin films. High-throughput 3D phase-field simulations were performed to construct the parametric relationship among the process/model parameters and the film properties. The optimal parameters were further investigated using a novel hierarchical multi-objective optimization strategy. Nevertheless, the crystalline orientation was not considered in Ref. [2, 4], which cannot give a precise description of the growth of polycrystalline films.

Consequently, 3D quantitative phase-field simulations of microstructure evolution of polycrystalline Ti thin films prepared by PVD were conducted in this research. This research employed a phase-field model based on the results in Ref. [35–36] with a moving frame strategy for simulation of PVD polycrystalline films. Additionally, the model parameters based on Ref. [2] were investigated, and 3D quantitative simulations of grain growth and evolution of PVD Ti thin films were performed. Finally, the influence of grain misorientation and deposition rate on the growth behavior of PVD Ti thin films was discussed.

2 Model and Simulation Settings

2.1 Phase-field model

In the practical PVD process, different stacking directions of atoms can lead to different orientations of columnar crystals. Grain boundary energy considering different orientations of grains should be introduced into the model. The phase-field model proposed by Ref. [35 – 36] can be employed to describe the grain evolution of single-phase polycrystalline films by coupling the interface growth phase-field model[20] and the solidification phase-field model of polycrystalline materials[21]. The main focus is related to PVD films: the deposition of vapor, the formation of solid phase on the surface, as well as the grain growth in polycrystalline materials. Three field variables are necessary to describe such a complicated process. Function $\phi(\boldsymbol{r},t)$ can be used to distinguish the deposited solid phase with $\phi(\boldsymbol{r},t)=1$ and gas region with $\phi(\boldsymbol{r},t)=-1$, and it can also describe the solid growth, where $\boldsymbol{r}$ is incident vapor direction, and t is time. Another variable $g(\boldsymbol{r},t)$ denotes the local density of the incident vapor. Besides, $g(\boldsymbol{r},t)=0$ indicates that there is no incident vapor. The third field variable $\theta(\boldsymbol{r},t)$ describes the misorientation of each grain within the domain. Therefore, the total free energy function over the spatial volume domain Ω depending on the grain misorientation can be given as follows:

$$F=\int_{\Omega}\left(-\frac{1}{2}\phi(\boldsymbol{r},t)^2+\frac{1}{4}\phi(\boldsymbol{r},t)^4+\alpha\left[\nabla\phi(\boldsymbol{r},t)\right]^2+sq\left[\phi(\boldsymbol{r},t)\right]\left|\nabla\theta(\boldsymbol{r},t)\right|+\frac{\varepsilon^2}{2}h\left[\phi(\boldsymbol{r},t)\right]\left|\nabla\theta(\boldsymbol{r},t)\right|^2\right)\mathrm{d}\Omega \tag{1}$$

where α, s, and ε are model parameters; q and h are functions. The initial two terms of Eq. (1) can define a double-well energy barrier between the equilibrium bulk solid and gas phases. The contribution of the existing solid-vapor interface to the overall free energy is introduced by the third term in Eq. (1), and the last two terms account for the contribution of grain misorientation. The functions $q[\phi(\boldsymbol{r},t)]$ and $h[\phi(\boldsymbol{r},t)]$ are required for crystalline orientation effects to be reduced or removed in a disordered region, respectively[35–36]. It is worth noting that the last two terms in Eq. (1) are required to consider the static grain boundary and grain boundary motion. The model parameters α, s, and ε in Eq. (1) depend on the feature size of grain boundary. The evolution of the field variable $\phi(\boldsymbol{r},t)$ is governed by the Allen-Cahn equation, and the variable $g(\boldsymbol{r},t)$ is governed by the Cahn-Hilliard equations[19], as follows:

$$\begin{aligned}\frac{\partial\phi}{\partial t}=&-\nabla^2\phi+\nabla^2\phi^3-2\alpha\nabla^4\phi+\nabla^2\left(s\phi\left|\nabla\theta\right|+\frac{\varepsilon^2}{2}\phi\left|\nabla\theta\right|^2\right)\\&+B\left(\nabla\phi\right)^2+C\sqrt{\left(\nabla\phi\right)^2}g\,\eta\end{aligned} \tag{2}$$

$$\frac{\partial g}{\partial t}=\nabla\left[D\nabla g-\boldsymbol{A}g\right]-B\left(\nabla\phi\right)^2 g \tag{3}$$

where ϕ, θ, and g are short terms for functions $\phi(\boldsymbol{r},t)$, $\theta(\boldsymbol{r},t)$, and $g(\boldsymbol{r},t)$, respectively; D is the diffusion velocity of vapor; B is an adjusting parameter to control the growth rate of thin films; $\boldsymbol{A}$ is the incident vapor vector; η is a Gaussian

distribution that provides surface fluctuations; C is a parameter to control the overall noise strength. The incident vapor vector $\boldsymbol{A}$ encompasses both the incident vapor strength A and the incident vapor direction $\boldsymbol{r}$ (i. e., $\boldsymbol{A}=A\boldsymbol{r}$). In Eq. (3), the first term represents the contribution of the diffusion of incident vapor, and the second term is responsible for the coevolution of gas and solid phases, including the consumption of incoming vapor and growth of the solid film.

The evolution of the non-conserved grain orientation is governed by the Allen-Cahn equation, which can be expressed as follows:

$$P\left(|\nabla\theta|\right)\tau_\theta\phi^2\frac{\partial\theta}{\partial t}=\nabla\cdot\left[\phi^2\left(\frac{s}{|\nabla\theta|}+\varepsilon^2\right)\nabla\theta\right] \tag{4}$$

where P indicates a function; τ_θ is relaxation constant. The kinetic process occurring at the grain interiors and grain boundaries is managed by the function $\mathrm{P}\left(|\nabla\theta|\right)$, as follows:

$$P\left(|\nabla\theta|\right)=1+\left(\frac{\mu}{\varepsilon}-1\right)\mathrm{e}^{-\beta\varepsilon|\nabla\theta|} \tag{5}$$

where β and μ are parameters to modulate the tendency for grain rotation and the migration rate of grain boundaries, respectively.

2.2 Numerical settings

In this research, the phase-field simulations were performed in a 3D domain with a size of 48 nm×48 nm×48 nm to save the computational resources. It is proven that the size of the simulation domain has restricted influence on the grain and surface morphology. The z-axis direction of the 3D simulation region is set as the film growth direction, and the incident vapor is deposited onto the substrate (z-axis). The periodic boundary condition is imposed along the substrate (x-axis and y-axis), the lower boundary of the direction perpendicular to the substrate (z-axis) is set as adiabatic boundary condition, and the upper side is set as a fixed boundary condition. At the beginning of the simulation, a substrate with thickness of 1/10 of the height of the simulated area should be set along the entire x-y plane. During PVD process, the supply of vapor and the growth of thin films were continuous. The moving frame strategy was adopted to focus on the vapor/solid interface. The rotation and combination of early formed grains can be considered as a grain evolution process without the growth of thin films. Therefore, the early-formed grains during the initial stage of PVD process were excluded from the simulation domain to simulate the real situation and improve the computational efficiency[2,4,37]. With the increase in film thickness, the simulation setting triggered the moving frame strategy when the film thickness increased to 3/5 of the height of the simulated area.

For the implementation of quantitative simulation of microstructure evolution of PVD Ti thin films, the explicit forward and centered finite difference methods with grid space dx=1.0 nm and time step dt=0.01 s were used to solve the governing equations with C++ code to enhance the computational efficiency.

3 Results and Discussion

3.1 Quantification of model parameters

The multiple parameters of PVD process, such as vacuum degree, working gas pressure, working gas purity, incident vapor, substrate materials/roughness/temperature, and deposition rate, have a significant impact on the microstructure of thin films[38–40]. For example, substrate temperature directly influences atomic surface diffusion and grain boundary migration rates, whereas working gas pressure affects the energy of sputtered particles and consequently the deposition rate. However, incorporating all these parameters simultaneously into a phase-field model with the consideration of grain orientation evolution, heat conduction, vapor transport, and gas-solid phase transformation presents substantial challenges in terms of both energy functional construction and numerical solution. In this research, the deposition rate, one of the most critical and controllable PVD parameters, was investigated, because it exerts a dominant influence on the resulting microstructure, film properties, and production efficiency[6,39]. Necessary simplification ensures the computational tractability and clarity of analysis, which also provides a basis for further research incorporating other process variables. Moreover, the incident vapor rate A regulates the quantity of vapor that reaches the thin film surface, while the coefficient B, which represents the gas-solid transition velocity, governs the transformation of the gas phase into a solid bulk phase in the interfacial domain. Thus, the deposition rate can be related to the model parameters A and B, according to the phase-field simulation results and the experiment data. Savaloni et al[41] reported that the Ti thin films tend to form an amorphous structure on glass with different deposition rates, while the incident angle is fairly large. It is also found that Ti thin films show the strongest texture with the deposition rate of 0.16 nm·s^{-1}. Then, it becomes weak with the further increase in deposition rate[41]. Therefore, 90 nm-thick Ti metal films can be deposited on Mo substrates with the deposition rate of 0.16 nm·s^{-1}. In this research, deposition rate of 1.02 nm·s^{-1} was used to explicate the effects of deposition rates and crystalline misorientation on the microstructure evolution of PVD Ti thin films[41]. Moreover, the non-vertical deposition was considered: the incident vapor tilt of 45° from the substrate surface (i.e., xoy-plane) was used in this research to more accurately simulate the experiment conditions[41]. Actually, the incident angles of incoming vapor reaching the substrate have a continuous distribution in PVD process. To simplify this process, a similar method was adopted to calculate the constant components of the flux $\boldsymbol{A}$ in the present PVD simulation, and three components are $\boldsymbol{A}_x=\boldsymbol{A}_y=\sqrt{2}/2\cos(a)A$ and $\boldsymbol{A}_z=\sin(a)A$, where a is the incident angle, and A is the incident vapor strength. The parameters g_0, β, μ, τ_θ, and ϵ are determined by the thermophysical parameters, and the detailed derivation of those parameters are described in Ref. [35–36]. Following the parametric strategy in Ref. [2], a large number of 3D simulation tests with consideration of crystalline

misorientation of PVD thin films using different deposition rates and model parameters were conducted in this research. The correspondence among the deposition rate, incident vapor rate, and gas-solid transition velocity can be obtained. Particularly, two corresponding sets of model parameters (summarized in Table 1) were adopted to perform quantitative 3D phase-field simulation of Ti thin films with the consideration of grain orientation. Moreover, it should be noted that the process parameters not considered in this research may lead to different model parameters, and the effects of these factors need further study in the future work.

3.2 Evolution of grain and grain misorientation in PVD Ti thin film

3D phase-field simulations with the model parameters listed in Table 1 were performed to investigate the evolution of grain and grain misorientation of PVD Ti thin films. The deposition rate of 0.16 $nm\cdot s^{-1}$ corresponds to the incident vapor rate of 2.087 $nm\cdot s^{-1}$ and the gas-solid transition velocity of 2.49 $nm^2\cdot s^{-1}$. It is well known that the roughness and surface structure of substrates have a significant influence on the nucleation sites and the initial stage of deposited thin film, which can further determine the initial grain orientations. In this research, the grain misorientations are randomly chosen from –10° to 10°.

Table 1 Model/material parameters used in 3D phase-field simulations

Parameter	Set 1	Set 2
Deposition rate/$m\cdot s^{-1}$	1.6×10^{-10}	1.02×10^{-9}
g_0	1.0	1.0
S/$J\cdot m^{-2}$	0.0176	0.1760
ϵ/$J\cdot m^{-1}$	1.41	1.41
$\tau_\theta/\times10^3$	1	1
$\mu/\times10^3$ $J\cdot m^{-1}$	1	1
$\beta/\times10^5$ $m^2\cdot J^{-1}$	1	1
a/$m^4\cdot s^{-1}$	0.5	0.5
$A/\times10^{-9}$ $m\cdot s^{-1}$	2.087	2.527
$B/\times10^{-18}$ $m^2\cdot s^{-1}$	2.49	3.53
D/$m^2\cdot s^{-1}$	1.0	2.0
C/$m\cdot s^{-1}$	2.5	2.5

The evolutions of the solid phase and grain misorientation obtained by the phase-field simulation are presented in Fig. 1. It can be seen that when the deposition rate is 0.16 $nm\cdot s^{-1}$, the deposited films are quite dense, and the surface roughness increases dramatically at the initial stage of PVD process and reaches a fairly steady value in the following stages. Moreover, it can also be found that a texture exists on the surface of thin films that is relevant to the incident angle of vapor, and this phenomenon conforms to the experiment results in Ref. [14,41]. Such a surface feature can be ascribed to the shadowing effect during PVD process. It is noted that most grains of deposited thin films have no significant change in crystallite size, compared with the randomly preset grains (6–10 nm in size). Grain evolution occurs through the grain boundary migration with the increase in thin film thickness, accompanied by the evolution of grain orientations. As shown in Fig. 1, the evolution of grain misorientations shows that the crystals of Ti thin films prefer to grow along with the initial orientation. Such a simulation result is reasonable, because it requires extra energy to induce the migration of grain boundary.

3.3 Effect of deposition rate and grain misorientation on growth of PVD Ti thin film

A series of 3D phase-field simulations were then performed using the model/material parameters listed in Table 1. To better understand the distinction between low-angle and high-angle grain boundaries, the simulations were conducted with randomly initial grain misorientation based on different ranges, such as from −5° to 5°, from −10° to 10°, and from −15° to 15°. Moreover, a set of simulations with quite narrow grain misorientation range from − 0.1° to 0.1° were also adopted for a direct comparison to explicate the effect of crystalline orientation on the microstructure evolution during PVD process of Ti thin films.

Fig. 2 shows the evolution of Ti thin film grains with

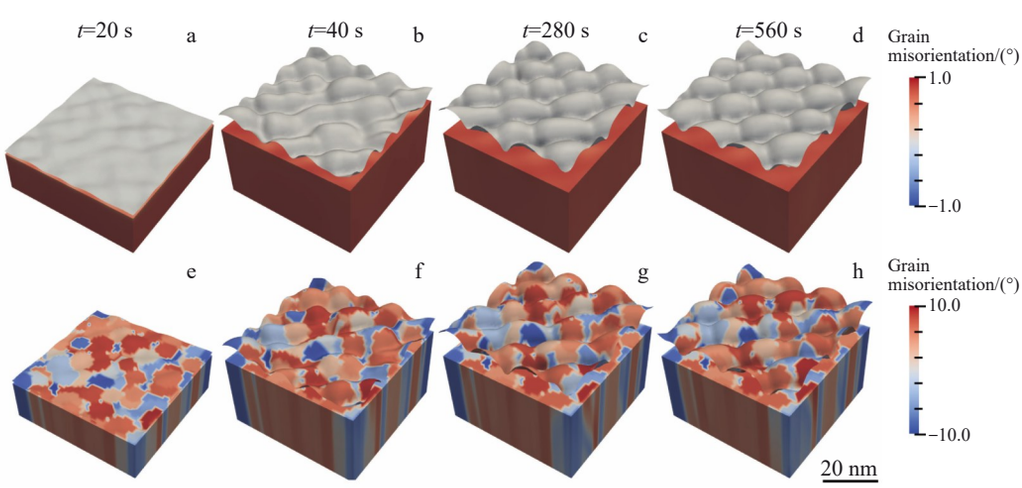

Fig.1 Phase-field simulated microstructure evolutions of Ti thin films deposited at deposition rate of 0.16 $nm\cdot s^{-1}$ and initial grain misorientation range from −10° to +10°: (a–d) phase evolutions; (e–h) grain misorientation evolutions

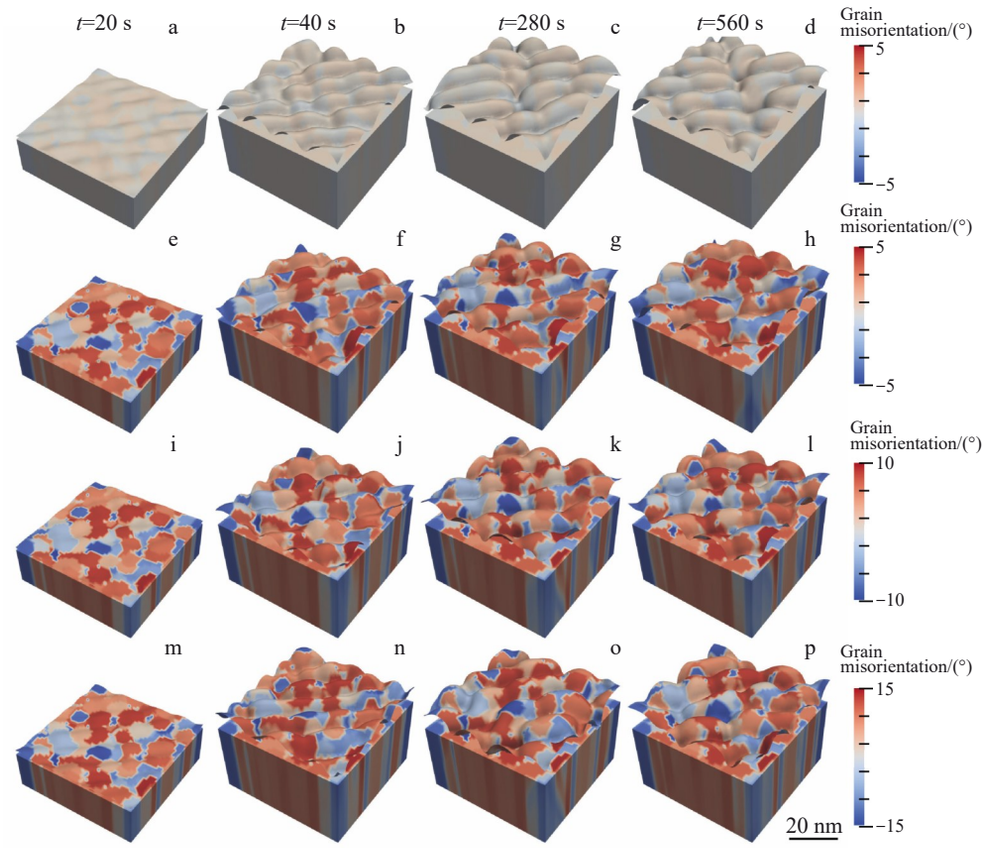

Fig.2 3D phase-field simulations of evolutions of local grain misorientations of Ti thin films deposited at deposition rate of 0.16 nm·s^{-1} with different grain misorientations at t=20 s (a, e, i, m), t=40 s (b, f, j, n), t=280 s (c, g, k, o), and t=560 s (d, h, l, p): (a–d) from −0.1° to 0.1°; (e–h) from −5° to 5°; (i–l) from −10° to 10°; (m–p) from −15° to 15°

different initial grain misorientations during PVD from 20 s to 560 s. It shows that the Ti thin films grow along the presupposed orientations rapidly, and there is no significant change in crystallite size. The other interesting feature lies in the fact that the Ti thin films grow without the consideration of grain misorientation, showing a prominently textured surface. The continuous domains and tilted micro-columns are formed and inclined toward the vapor direction. However, such a textured surface of polycrystalline Ti thin films becomes inconspicuous with the increase in grain misorientation. A discontinuous polycrystalline surface can be found in PVD Ti thin films with higher initial grain misorientation. This phenomenon fits well with the experiment observations[14]. Moreover, according to Ref. [14], its intrinsic mechanism can be ascribed to the growth habits of nuclei, which further control the evolution of crystallite growth. With the increase in grain misorientation, the grains prefer to grow with the same orientation as that of the initial grains, and the combination of different grains becomes fairly difficult due to the higher energy barrier. Therefore, it may reduce the shadowing effects by controlling the initial nucleation orientation of polycrystalline Ti thin films.

The evolution of local grain misorientations with different deposition rates and initial grain orientations is presented in Fig. 3. It is seen that the roughness of Ti thin films increases more quickly at the initial stage when the deposition rate changes from 0.16 nm·s^{-1} to 1.02 nm·s^{-1}. Moreover, it seems that the deposition rate has no significant influence on the grain growth, and the grains have similar misorientation at the initial stage whether the deposition rate is 0.16 or 1.02 nm·s^{-1}. It is obvious that a weak preferred orientation of the surface texture of Ti thin films exists with the increase in deposition rate. The surface texture can be eliminated with the increase in grain misorientation when the deposition rate is 1.02 nm·s^{-1}. The effects of deposition rate and grain misorientation on the surface are demonstrated in Fig.4–Fig.5. It is obvious that the surface roughness of the Ti thin films deposited with different grain misorientations is fairly small within the first 20 s, and it increases when the deposition further proceeds from 20 s to 280 s, but it fluctuates around a specific value from 280 s to 560 s. This result indicates that the growth process of Ti thin film lasts approximately 280 s to achieve a stable state when the deposition rate is 0.16 nm·s^{-1}. Moreover, at the deposition rate of 0.16 nm·s^{-1}, the wave-like surface texture is more visible with small initial grain orientation (Fig. 4), because of the continual incorporation of micro-columnar grains and the shadowing effect during PVD process. As the deposition rate increases to 1.02 nm·s^{-1}, the growth of Ti thin films can reach the steady state more quickly. According to Fig. 5, the surface heights increase to a steady value in the first 44 s, and intermittent micro-domains on the surface of thin films are more obvious. It is reported that the adatoms are becoming

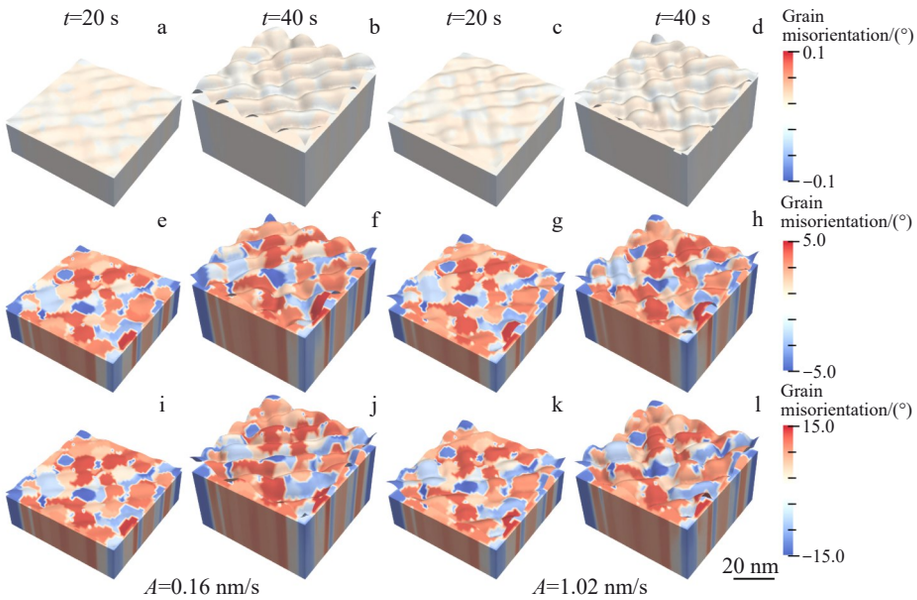

Fig.3 Evolution of local grain misorientations of Ti thin films deposited at deposition rate of 0.16 nm·s^{-1} (a – b, e – f, i – j) and 1.02 nm·s^{-1} (c–d, g–h, k–l) with different grain misorientations at t=20 s (a, c, e, g, i, k) and t=40 s (b, d, f, h, j, l): (a–d) from −0.1° to 0.1°; (e–h) from −5° to 5°; (i–l) from −15° to 15°

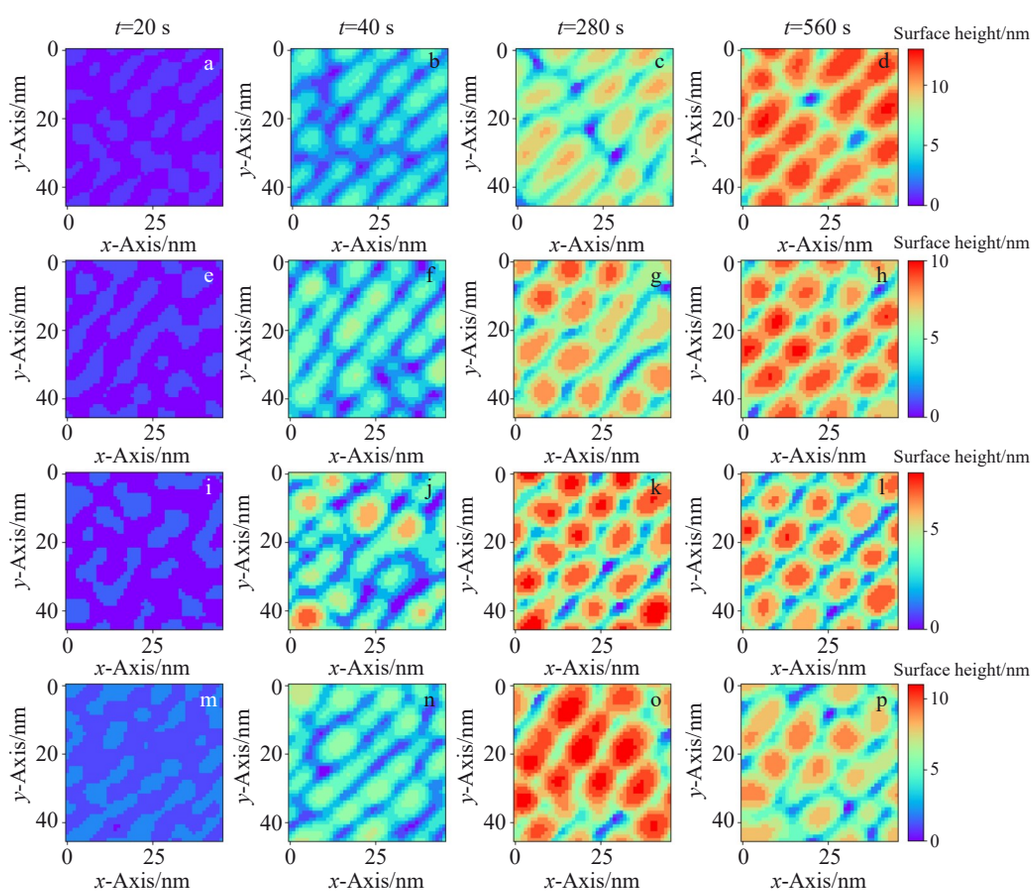

Fig.4 3D phase-field simulated heat maps of surface height of Ti thin films deposited at deposition rate of 0.16 nm·s^{-1} with different grain misorientations at t=20 s (a, e, i, m), t=40 s (b, f, j, n), t=280 s (c, g, k, o), and t=560 s (d, h, l, p): (a–d) from −0.1° to 0.1°; (e–h) from −5° to 5°; (i–l) from −10° to 10°; (m–p) from −15° to 15°

increasingly localized to their designated landing areas if the deposition rate is faster than a critical point[41]. Thus, the growth process of Ti thin films with faster deposition rate depends on the nucleation of the domains, while the initial

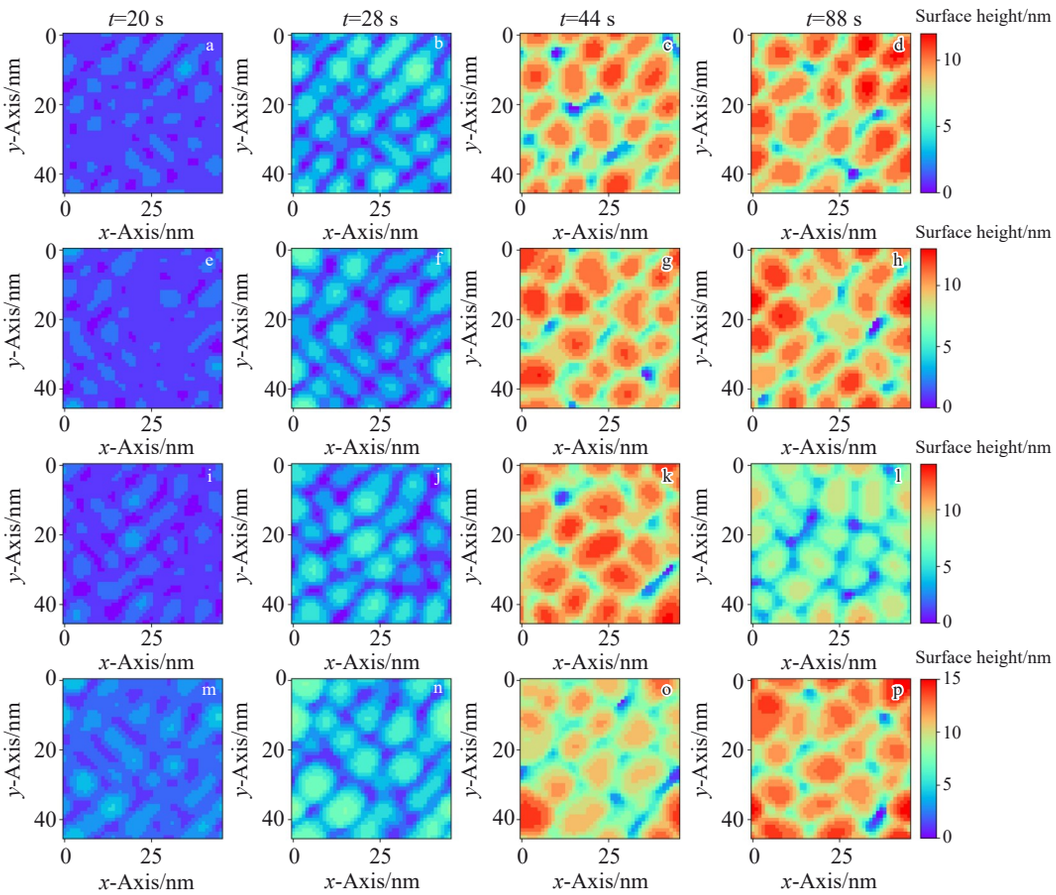

Fig.5 3D phase-field simulated heat maps of surface height of Ti thin films deposited at deposition rate of 1.02 nm·s^{-1} with different grain misorientations at t=20 s (a, e, i, m), t=28 s (b, f, j, n), t=44 s (c, g, k, o), and t=88 s (d, h, l, p): (a–d) from −0.1° to 0.1°; (e–h) from −5° to 5°; (i–l) from −10° to 10°; (m–p) from −15° to 15°

grain misorientations are randomly generated in this phase-field simulations. Comparing Fig.4 with Fig.5, it can be found that the surface heights of Ti thin film increase slightly when the deposition rate increases from 0.16 nm·s^{-1} to 1.02 nm·s^{-1}. This is due to the lack of sufficient time for the vapor to adequately spread out and fluctuate with a fairly fast deposition rate and a gas-solid transition velocity.

To make a comprehensive comparison between the simulated and the experimental results, experiment data from Ref.[41] were used. The most frequently used parameters for quantifying the surface roughness (i.e., the arithmetic average roughness R_a and the root mean square roughness R_q) were calculated based on the 3D phase-field simulated microstructures. The calculations of parameters R_a and R_q can be performed using the following equations:

$$R_a = \frac{1}{N_x \cdot N_y} \sum_{j=1}^{N_y} \sum_{i=1}^{N_x} \left| Z_{ij} - \mu \right| \tag{6}$$

$$R_q = \sqrt{\frac{1}{N_x \cdot N_y} \sum_{j=1}^{N_y} \sum_{i=1}^{N_x} \left(Z_{ij} - \mu \right)^2} \tag{7}$$

$$\mu = \frac{1}{N_x \cdot N_y} \sum_{j=1}^{N_y} \sum_{i=1}^{N_x} Z_{ij} \tag{8}$$

where $N_x \cdot N_y$ represents the size of the data sample; Z_{ij} is an array to map the topography of the thin film surface in the x-y plane, providing valuable information about the relative heights; μ is the mean value of relative surface heights. The simulated and experimental results are shown in Fig. 6. The values of R_a and R_q increase rapidly in the initial stage at the deposition rate of 0.16 nm·s^{-1} and then achieve a stable state after 90 s with the average thickness about 14.4 nm. At the deposition rate of 1.02 nm·s^{-1}, the steady state is reached earlier. As shown in Fig. 6, the values of R_a and R_q slightly increase with the influence of grain misorientation. It is found that the great majority of R_a/R_q ratios converge to a value close to 1.30, inferring that the distribution of surface heights of Ti thin films closely resembles a Gaussian distribution, which aligns well with the results in Ref. [42]. Additionally, the calculated values of R_a and R_q of Ti thin films at the deposition rate of 0.16 nm·s^{-1} after 560 s are approximately 1.48 and 1.80 nm, presenting a good consistency with the experimental data of 1.50 and 1.96 nm[41], respectively. Meanwhile, the simulated R_a and R_q values of Ti thin films at the deposition rate of 1.02 nm·s^{-1} with different grain misorientations are approximately 1.55 and 1.95 nm, which are slightly larger than the experimental data of 1.36 and 1.79 nm[41], respectively. It can be found that the experimental surface

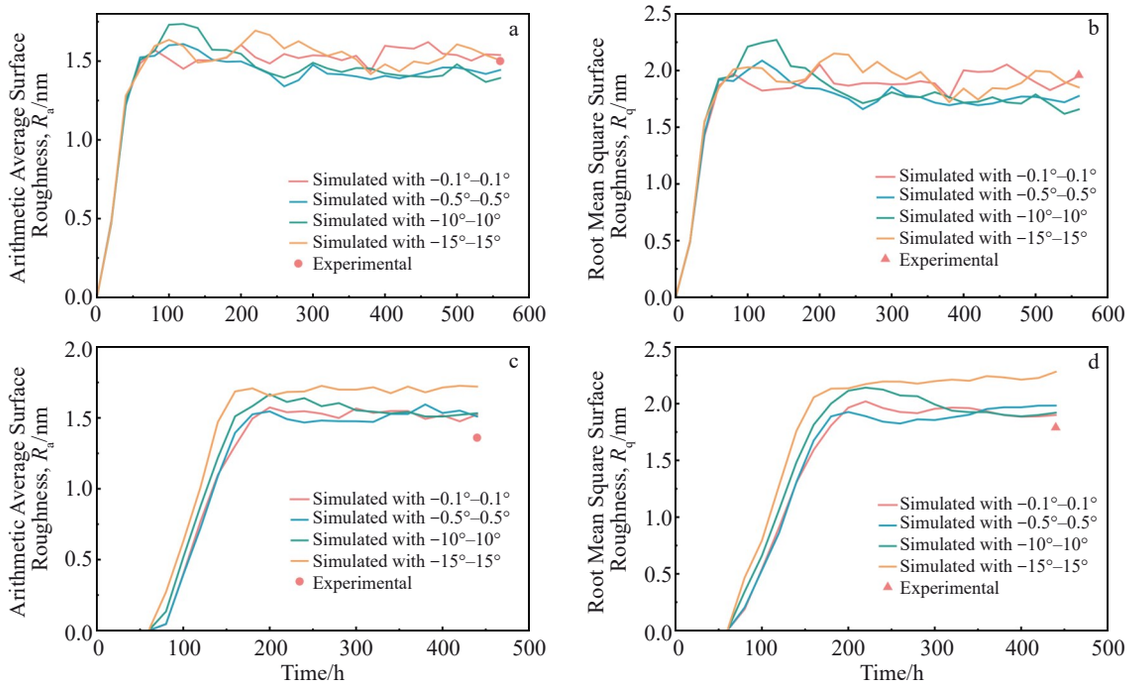

Fig.6 Comparison between simulated and experimental results of arithmetic average surface roughness R_a (a, c) and root mean square surface roughness R_q (b, d) for Ti thin films during PVD with different grain misorientations at deposition rate of 0.16 nm·s^{-1} (a–b) and 1.02 nm·s^{-1} (c–d)

roughness is decreased with the increase in deposition rate. At faster deposition rates, the deposited particles can be buried under a thick layer of incoming atoms, which can restrain the diffusion of adatoms. Thus, more new nuclei tend to form and further produce a closed pack fibrous structure[41,43]. In this research, however, the number of nuclei at different deposition rates is specified as the same value to study the effect of grain misorientation on the morphologies of PVD Ti thin films. The vapor on the surface of PVD Ti thin film does not have sufficient time to adequately diffuse and fluctuate, and the shadowing effects are more obvious. Therefore, the simulated surface roughness is slightly larger than the experimental one, but the discrepancy is still within the margin of error.

4 Conclusions

1) The 3D phase-field model coupling with the moving frame strategy can be used for the simulation of PVD polycrystalline films. Multiple model parameters (incident vapor rates and gas-solid transition velocities) corresponding to various deposition rates can be quantified through numerous 3D phase-field simulation tests of grain evolution of PVD thin films.

2) The crystals of Ti thin films prefer to grow along with the initial orientation, and there is no significant change in crystallite size.

3) A strong surface texture exists on the surface of Ti thin films deposited at slow deposition rate, and the surface texture can be eliminated with the increase in deposition rate and initial grain orientation. Moreover, the grain misorientation can increase the surface roughness of the Ti thin films. The simulated surface roughness shows a good agreement with the experimental one.

4) This research indicates that the presently used phase-field model and quantification method are feasible for the investigation of grain evolution of other polycrystalline metal thin films, which is anticipated to give a more precise description of microstructure evolution in different PVD polycrystalline films.

References

1 Mattox D M. *Handbook of Physical Vapor Deposition Processing*[M]. Oxford: William Andrew, 2010

2 Yang S L, Zhong J, Chen M *et al*. *Coatings*[J], 2019, 9(10): 607

3 Rossnagel S M. *Journal of Vacuum Science & Technology A*[J], 2020, 38(6): 060805

4 Dai R, Yang S, Zhang T *et al*. *Frontiers in Materials*[J], 2022, 9: 924294

5 Zhong Zhiqiang, Chen Yi, Xue Yan *et al*. *Rare Metal Materials and Engineering*[J], 2025, 54(6): 1620 (in Chinese)

6 Suliali N J, Goosen W E, Janse V V A *et al*. *Vacuum*[J], 2022, 195: 110698

7 Liang S X, Liu K Y, Yin L X *et al*. *Journal of Vacuum Science & Technology A*[J], 2022, 40(3): 030801

8 Lüdecke C, Bossert J, Roth M *et al*. *Applied Surface Science*[J], 2013, 280: 578

9 Sultana T, Newaz G, Georgiev G L *et al*. *Thin Solid Films*[J], 2010, 518(10): 2632

10 Qin W, Chen M, Wang Y R *et al*. *Computational Materials Science*[J], 2020, 174: 109504
11 Gablech I, Svatoš V, Caha O *et al*. *Journal of Materials Science*[J], 2016, 51(7): 3329
12 Fazio M, Vega D, Kleiman A *et al*. *Thin Solid Films*[J], 2015, 593: 110
13 Mahieu S, Ghekiere P, Depla D *et al*. *Thin Solid Films*[J], 2006, 515(4): 1229
14 Sadeghi-Khosravieh S, Robbie K. *Thin Solid Films*[J], 2017, 627: 69
15 Naoe M, Ono S, Hirata T. *Materials Science and Engineering A*[J], 1991, 134: 1292
16 Hoshi Y, Suzuki E, Shimizu H. *Electrochimica Acta*[J], 1999, 44(21–22): 3945
17 Chinaglia E F, Oppenheim I C. *MRS Proceedings*[J], 2001, 672: O3.26
18 Astinchap B. *Optik*[J], 2019, 178: 231
19 Gablech I, Caha O, Svatoš V *et al*. *Thin Solid Films*[J], 2017, 638: 57
20 Keblinski P, Maritan A, Toigo F *et al*. *Physical Review E*[J], 1996, 53(1): 759
21 Warren J A, Kobayashi R, Lobkovsky A E *et al*. *Acta Materialia*[J], 2003, 51(20): 6035
22 Stewart J A. *Computational Materials Science*[J], 2022, 211: 111503
23 Zhao Y H, Liu K X, Hou H B *et al*. *Materials & Design*[J], 2022, 216: 110555
24 Chen L Q, Zhao Y. *Progress in Materials Science*[J], 2022, 124: 100868
25 Zhao Y H, Xing H, Zhang L J *et al*. *Acta Metallurgica Sinica* (*English Letters*)[J], 2023, 36(11): 1749
26 Zhao Y H. *npj Computational Materials*[J], 2023, 9(1): 94
27 Zhang T D, Zhong J, Zhang L J. *MRS Communications*[J], 2023, 13(5): 877
28 Zhang T D, Zhong J, Zhang L J. *Computational Materials Science*[J], 2024, 244: 113260.
29 Long Y H, Zhong J, Zhang T D *et al*. *Computers, Materials and Continua*[J], 2024, 79(3): 3435
30 Peng W, Li X, Gao J B *et al*. *Acta Materialia*[J], 2024, 276: 120141
31 Ma S, Liu P C, Zhang L J. *Journal of Nuclear Materials*[J], 2025, 603: 155413
32 Zhao Y H, Xin T Z, Tang S *et al*. *MRS Bulletin*[J], 2024, 49(6): 613
33 Pei Jiaqi, Hou Hua, Yang Wenquan *et al*. *Rare Metal Materials and Engineering*[J], 2024, 53(3): 834 (in Chinese)
34 Hao Mengyuan, Li Pei, Wang Dong. *Materials China*[J], 2022, 41(7): 497 (in Chinese)
35 Stewart J A, Spearot D E. *Computational Materials Science*[J], 2016, 123: 111
36 Stewart J A, Spearot D E. *Computational Materials Science*[J], 2017, 131: 170
37 Zhang L J, Stratmann M, Du Y *et al*. *Acta Materialia*[J], 2015, 88: 156
38 Grovenor C R M, Hentzell H T G, Smith D A. *Acta Metallurgica*[J], 1984, 32(5): 773
39 Cai K, Müller M, Bossert J *et al*. *Applied Surface Science*[J], 2005, 250(1): 252
40 Achour A, Lucio-Porto R, Chaker M *et al*. *Electrochemistry Communications*[J], 2017, 77: 40
41 Savaloni H, Reissi M H, Shariati M *et al*. *Thin Solid Films*[J], 2006, 515(2): 439
42 Thomas T R. *Rough Surface*[M]. New York: Imperial College Press, 1998
43 Savaloni H, Player M A. *Vacuum*[J], 1995, 46(2): 167

纯 Ti 薄膜物理气相沉积过程中晶粒演化三维定量相场模拟

张童弟[1]，马　飒[1,2]，钟　静[1]，杨胜兰[1,3]，张利军[1]
(1. 中南大学 粉末冶金全国重点实验室，湖南 长沙 410083)
(2. 浙江大学 材料科学与工程学院，浙江 杭州 310027)
(3. 重庆大学 国家镁合金材料工程技术研究中心，重庆 400044)

摘　要：结合相场方法和移动边界方法，对不同沉积速率和晶粒取向下物理气相沉积Ti薄膜的生长和晶粒演化进行了三维相场模拟，同时考虑了其形貌和晶粒取向的演化。模拟结果表明：在较低沉积速率下形成的Ti薄膜表面存在明显取向的纹理结构，Ti薄膜表面粗糙度与晶粒取向差呈正相关；同时，模拟获得的表面粗糙度与实验结果吻合较好。

关键词：物理气相沉积；相场模拟；晶粒演化；多晶；Ti薄膜

作者简介：张童弟，男，1997年生，博士生，中南大学粉末冶金全国重点实验室，湖南 长沙 410083，E-mail：tongdiz@csu.edu.cn